Ocean Waves Measurement and Analysis, Fifth International Symposium WAVES 2005, 3rd-7th, July, 2005. Madrid, Spain
Paper number: 134

Please note the existence of additional information at the end of this publication on resonant basin oscillations referring to page 7 and to Fig.08. Due to the author´s finding of a phase jump (2010), existing at steep slopes, the respective natural basin frequencies should be calculated considering the real boundary conditions by applying an uneven number of quarter wave lengths.

WAVE RESONANCES DETECTED IN A WAVE TANK AND IN THE FIELD

Fritz Buesching[1]

Abstract: At Sylt Island/Germany, boundary conditions formed by a structured long shore bar, running roughly parallel to the shoreline, are found to be the reason for intense resonance absorption effects at storm surge conditions. Incoming waves interact with the water level deflections in the trough located between the bar and the beach in such a way that frequency components match a limited number of possible harmonics of the enclosed body of water. As there are significant energy densities to be found in the wave energy spectra at harmonic numbers 1 through 3 of the enclosed water body, this phenomenon is believed to be responsible for the tremendous coastal recessions at this island due to storm surge occurrences in the past. The existence of *resonant seiching* modes is deduced from intense low frequency *anomalous dispersion effects* (ADE), which had been found in the 1970s. Such effects - well known from *resonant absorption of electromagnetic waves* - recently also could be verified in a wave tank. Using a special technique of analysing composite spectra (containing information of incoming, reflected and re-reflected waves), it was possible to detect a set of partial standing waves existing simultaneously. As each partial clapotis is composed of a number of neighbouring frequency components comprising of nearly equal wave length, such components must obey an anomalous dispersion law dc/df > 0.

INTRODUCTION

The term *wave resonance* often is used in connection with the *Bragg Scattering Phenomenon,* originally observed in X-ray-crystallography by the Bragg brothers in 1913. With respect to shallow water waves Heathershaw (1982) impressively demonstrated that, at so-called *Bragg resonance*, a partially standing wave forms on the seaward side of a series of long-shore sandbars, linearly changing into a propagating wave at the landward side of the sandbar configuration. In particular a significant increase in reflected wave energy is due to multiple backscattering from neighboring bars, if the incident progressive waves are twice as long as the bar spacing. See also Mei (1989) and others.

By contrast the present study focuses on boundary conditions different from a periodic series of long-shore sandbars, i.e. a configuration merely consisting of a *single*

1 Professor Dr.-Ing., Bielefeld University of Applied Sciences, HYDROMECH, Diesselhorststr. 01, D-38116 Braunschweig, Germany, buesching@hollow-cubes.de

sandbar running roughly parallel to the shoreline with the waves reflecting in-between. Actually the water body in the trough between the bar and the beach is looked upon as a resonator, which is able to execute different modes of natural oscillations; the resonator incited by the incident waves arriving from sea.

Nevertheless the author also refers to resonance phenomena known from electromagnetic waves (EM-waves): As is well known, both *air* and *water* exhibit strong resonant absorption of EM-waves in both the ultraviolet and infrared regions of the spectrum. The significant circumstances can best be demonstrated by the behaviour of the complex dielectric constant $\varepsilon_r = \mathrm{Re}[\varepsilon] + i \cdot \mathrm{Im}[\varepsilon]$, which nearly corresponds to the square of the complex refractive index $N = n + ik$. In Fig.01 the real and the imaginary part of the dielectric constant are plotted along with frequency. The real part Re[ε] describes the dispersion property (dε/df), whereas the imaginary part Im[ε] represents an absorption quantity. It is well known, that the definition of the normal dispersion

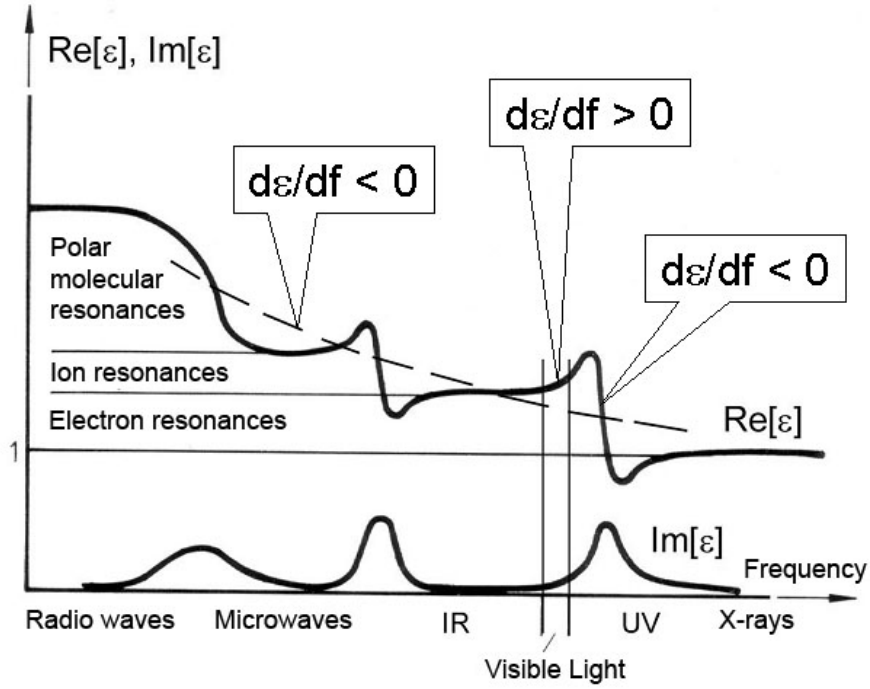

Fig.01. Resonant Absorption of EM-Waves: Real and Imaginary Components of the Complex Dielectric Constant ε (schematically).

(representing the normal sequence of spectral colours according to $dn/df > 0$ or $d\varepsilon/df > 0$ respectively) stems from observations in the very narrow *visible* frequency band (merely comprising 2% of the total electromagnetic spectrum). It is, however, obvious, that the dispersion globally is anomalous in the range between long radio waves and high frequency X-rays, see dashed line. But most impressively the spots of resonance are assigned by maxima of the imaginary part and by oscillations of the real part of the dielectric constant, i.e. by strong anomalous dispersion ($d\varepsilon/df << 0$) neighboured by maxima and minima right next to the resonance frequency. Therefore the statement applies that *resonance, absorption* and *anomalous dispersion* are inextricably connected phenomena. The one can not exist without the others.
In the figure shown the strong anomalous dispersion effects are due to *ion-resonances* in the IR-range and due to *electron-resonances* in the UV-range. Hence, the maxima of absorption at the same time represent maxima of energies, which are due to the

interaction of the exciting waves with ion-resonators or electron-resonators respectively.

In the remainder of this publication an analogue correlation of such phenomena also will be discussed for *gravity waves* in a wave tank (model) as well as in the field. In both cases the resonators are formed by confined water bodies, which are able to execute different modes of natural oscillations. Because of the lack of space here, the field measurements can not be addressed in detail. Missing information and additional discussion and conclusions can be found in Büsching (2003).

WAVE RESONANCE PHENOMENA IN A WAVE TANK

Model investigations had been carried out in a wave tank of Bielefeld University of Applied Sciences (BUAS), see Fig.02.

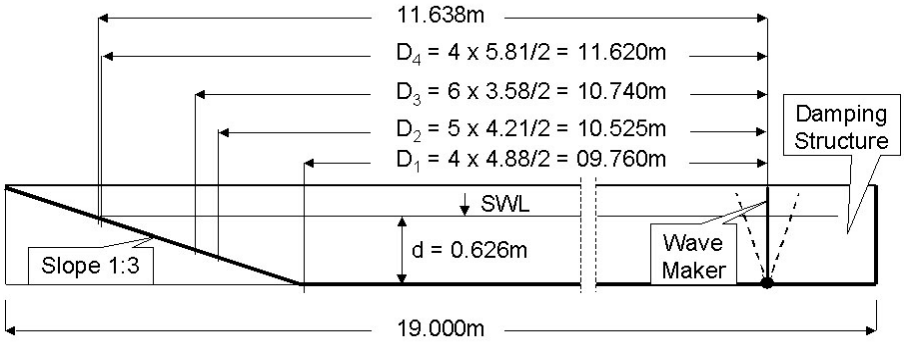

Fig. 02. BUAS Wave Tank (schematically). Different Distances D_i with Respect to the Hinge of the Flap are explained further below.

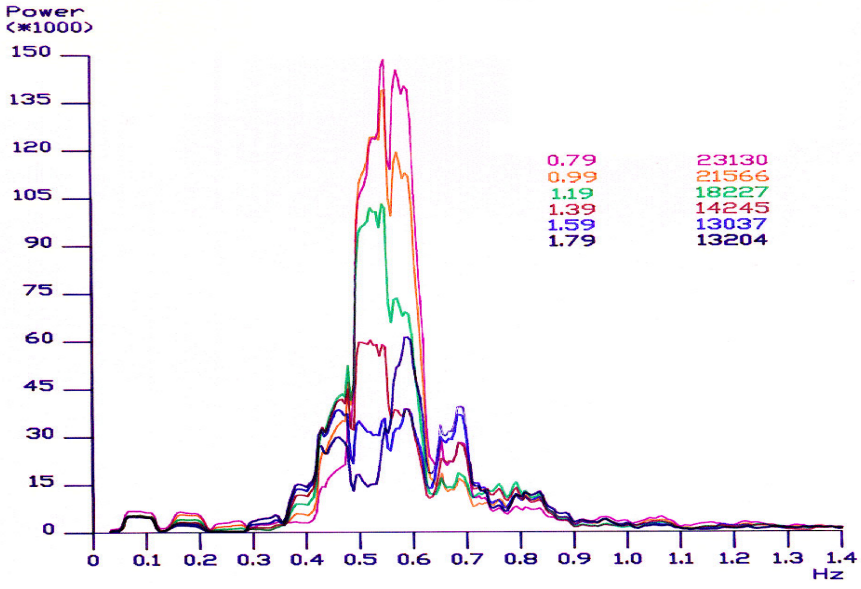

Fig. 03. Synchronously Measured Energy Spectra in Front of a Plane Revetment Structure at Slope 1:3.

The actual evaluations refer to the boundary conditions of a smooth slope inclined 1:3 and a rigid flap type wave generator, at which an input spectrum was used, whose frequency range - scaled up to prototype - resembled those measured at the beach stations on Sylt Island, see Fig.10 (Büsching 1975, 1976).

In order to favor the development of high energetic movements in the tank, in this case, no precautions had been made to suppress *re-reflection* from the wave maker. The

tests had been carried out comprising a rather big number of 91 wave probe stations positioned in front of the slope from station 0,79m to 9.79m, equally spaced 10cm, nearly all over the total length of the wave tank. The signals from the wave probes were recorded quasi synchronously and were processed by spectrum analyses confined to a total frequency range $0.03263 \le f \le 1.3997$ Hz. As an example in Fig.03 there are plots of spectra synchronously taken at 6 different gage locations, spaced 20cm, in front of the smooth plane slope. Actually those *composite* energy spectra (containing information of incoming waves, reflected waves and re-reflected waves) demonstrate the changes of energy content along the slope in the range extending from the slope toe (station 1.79m) to the zone of maximum breaker instability (stations 1.19m to 0.79m).

In the following 3 diagrams (Fig.04 – Fig.06) the values of all the integrated spectra IA (variance) are plotted along with the gauge station distance from the slope face, i.e., from the point IP of the still water level (SWL) intersecting the slope, which is also sketched in relation to the probe stations at the bottom of Fig.04.

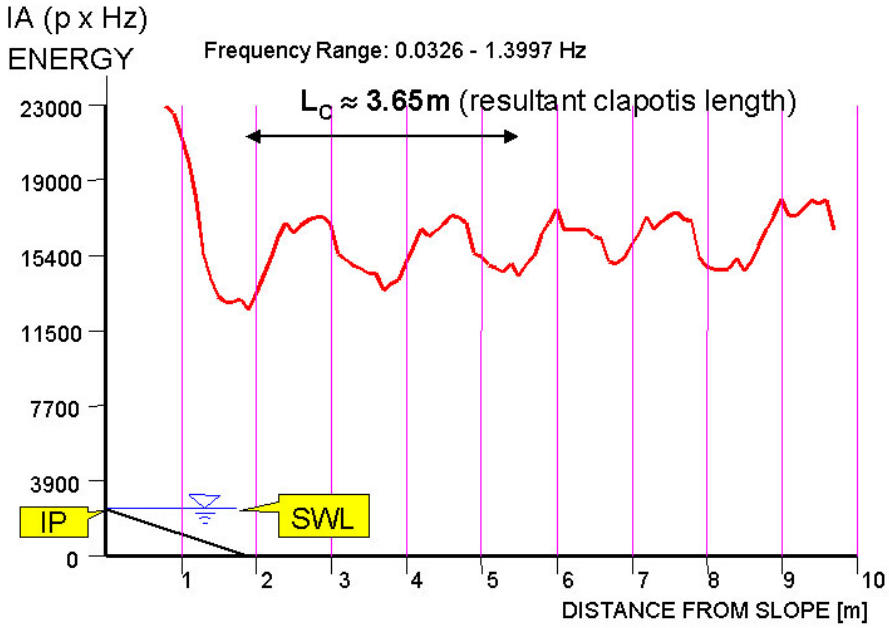

Fig. 04: Integral Values of Spectral Energy within $0.03 \le f \le 1.4$ Hz, Documenting the Existence of a Partial Clapotis in Front of the Slope 1:3.

Because the variance is proportional to the wave energy (of vertical water level deflections) contained in the respective frequency range, changes in those plots can be interpreted with respect to the actual position and dominance of a possible *partial standing wave (partial clapotis)* in relation to the sloping structure.

In Fig.04 the variation in the plot of the total energy indicates that the length of a "resultant partial Clapotis" is about $L_C = 3.65$m (distance between the first and third minimum of energy). Although there are some disturbances to be seen in the plot, it will be shown that conclusions of good quality can be drawn from that data, provided that the total frequency range is subdivided into a number of smaller frequency ranges and the higher noise frequencies ($f > 1$ Hz) are discarded.

Because of insufficient graphic resolution, a respective presentation of all 256 frequency components separately (spaced $\Delta f = 0.00543$ Hz) was abandoned. The *essential* phenomenon, however, comes out clearly enough from Fig.05, where about 60 lines of energy relating to enlarged frequency intervals ($n \cdot \Delta f$) are calculated for a confined frequency range $0.45\text{Hz} \le f \le 0.66$ Hz.

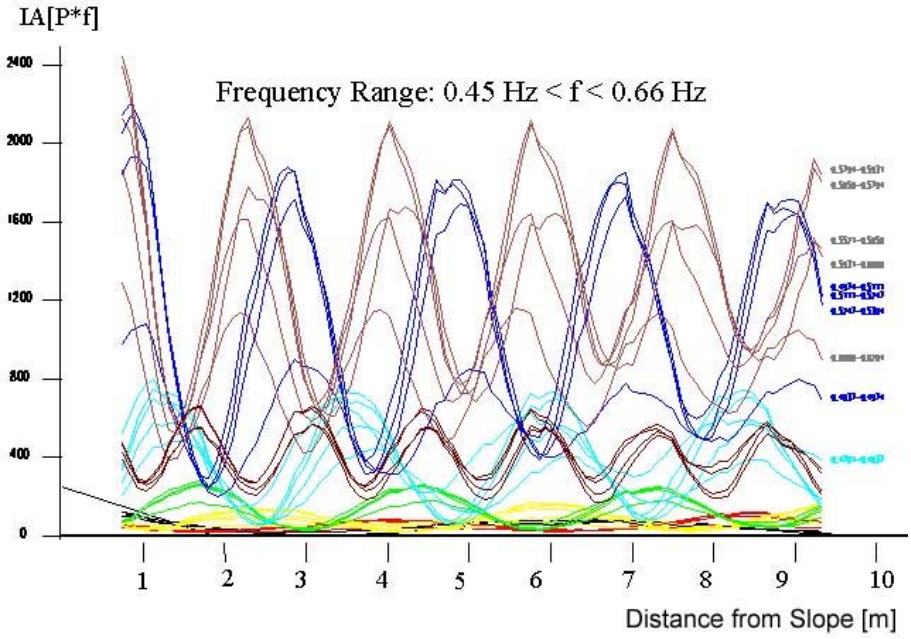

Fig. 05: Energy Enclosed in Enlarged Energy Containing Frequency Intervals.

It can be seen clearly that there are lines of energy, possessing *similar* energy distributions in the length expansion, relating to the distance from the sloping structure (point IP); i.e., they have nearly same distances between neighbouring energy minima or neighbouring energy maxima respectively and nearly same phase angles.

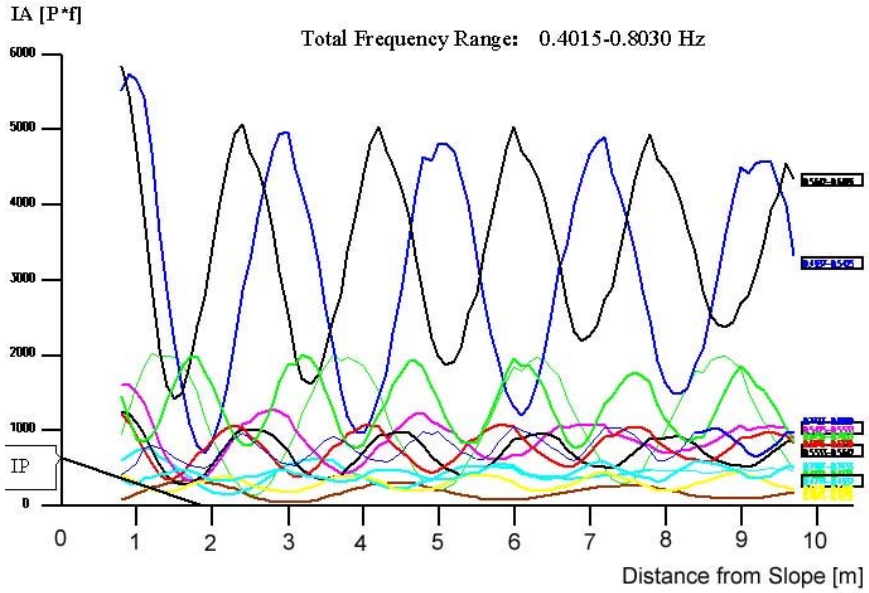

Fig. 06: Energy Content of 12 Definable Partial Standing Waves

With respect to the frequency range 0.4015 Hz ≤ f ≤ 0.8030 Hz 82 *energy lines* were found, which could be assigned to 12 different partial clapotis lengths corresponding to 12 definable sub-frequency ranges, see Fig.06. Thus the partial clapotis, documented in Fig.04, can be recognized approximately as the resulting wave from 12 superimposing partial clapotis waves existing in the wave tank synchronously. In order to distinguish the resultant partial clapotis from its components in the

following the latter shall be named shortly "partial waves". The general properties of such partial waves can be derived from their energy distribution in the length expansion (energy line) as shown in Fig.07.

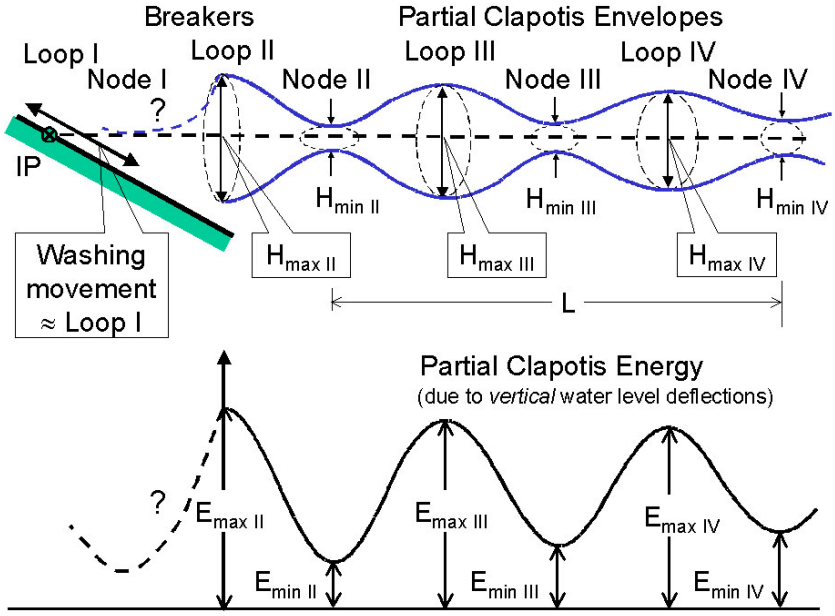

Fig. 07: Sketch of Partial Standing Wave at a Slope.

The particle movements at phases of the loops can be approximated by ellipses possessing *bigger vertical* principle axis and those at the node phases by ellipses possessing *bigger horizontal* principle axis. The orbital motions of partial waves *approaching* the slope may be described by *increasing* vertical ellipse axis at the loops and *decreasing* vertical ellipse axis at the nodes. Based on the respective 12 energy lines the author previously had published additional information on *increasing reflection coefficients with frequencies decreasing* (Büsching, 1992) and *on the relative deformation of the partial clapotis waves approaching the slope* (Büsching, 2001).

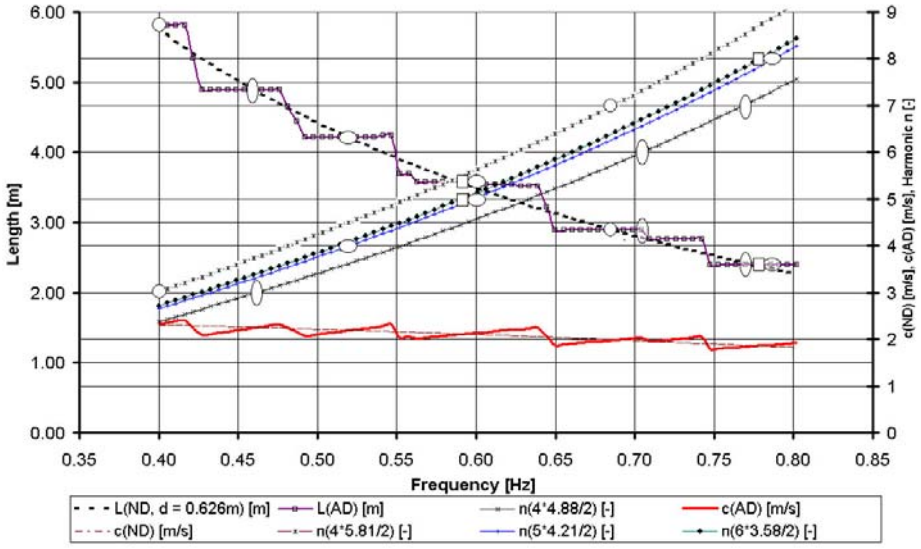

Fig. 08: Component Lengths L, Phase Velocities c and Harmonic Numbers n Plotted with Frequency.

The most striking outcome, however, with respect to the above data analysis, is the fact that partial waves – comprising of nearly *equal component lengths* - must obey an *anomalous dispersion law dc/df > 0*, because (at water depth being constant) the phase velocity $c = L \cdot f$ *increases* with frequency, see lower red curve of Fig.08.

In the upper part of Fig.08 the lengths associated with the 82 energy lines, mentioned above, are denoted L(AD)(f) (AD = anomalous dispersion), whereas L(ND)(f) (ND = normal dispersion; dashed line) refers to the classical dispersion relation according to water depth d = 0.626 m in the wave tank. Both curves can be named *Length Spectra*. Besides the mentioned (red) phase velocity spectrum c(AD)(f) also the theoretical phase velocity spectrum c(ND)(f) is shown in the lower part of the figure.

Because of the stepped structure of L(AD)(f), suggesting the existence of different oscillatory modes of the enclosed water body in the tank synchronously, in the following it will be shown that boundary conditions are compatible with higher harmonics. Natural frequencies of a water volume in a basin comprising of vertical walls can be calculated in using Merian´s formula (01):

$$f\,[Hz] = (n+1) \cdot \frac{c}{2 \cdot D} \qquad (01)$$

where D = horizontal wall distance; c = wave celerity; n = harmonic number. n = 0 denotes the fundamental oscillation and n = 1, 2, 3...are named first, second, third harmonic etc. Solving formula (01) with respect to harmonic numbers n[-], yields formula (02):

$$n(f)[-] = \frac{2 \cdot D \cdot f}{c} - 1 \qquad (02)$$

Applying $c = L \cdot f$ yields formula (03):

$$n(L)[-] = \frac{2 \cdot D}{L} - 1 \qquad (03)$$

At boundary conditions consisting of a slope at one side and a moving flap at the other (Fig.02) no distinct distance D can be suggested. That is why multiples of half-wave lengths of the 4 dominating longest partial waves (5.81m, 4.88m, 4.21m und 3.58m) were used in the formula together with the theoretical phase velocity, see Fig.02. As D_1 = 4 x 4.88/2 = 9.76m approximately equals the minimum distance between wave maker and the toe of the slope, the distances D_2 = 5 x 4.21/2 = 10.525m, D_3 = 6 x 3.58/2 = 10.74m and D_4 = 4 x 5.81/2 = 11.62m mark different points on the wet slope. Hence, according to such 4 distances there are also 4 different functions $n_i(f)$ in Fig.08. As a result it can be stated that the partial waves correspond to *higher* harmonic numbers $3 \le n \le 8$ of the enclosed water body. The fact that several harmonics obviously are linked by the *same* fundamental oscillation, actually confirms the existence of oscillatory modes pronounced by resonance. Thus intrinsic resonance frequency ranges are defined by frequency components comprising of *nearly equal* wave lengths. With respect to the function c(AD)(f) deviating distinctly from c(ND)(f) (Fig.08), the resonant components can be identified by the steps in the phase velocity function. *Portions of anomalous dispersion (dc/df > 0) are neighboured by portions of stronger normal dispersion (dc/df << 0).* It should be put stress on the fact that such a characteristic indeed resembles resonance features well known from EM-waves propagating through dielectrics, - although the frequency scales might be different, confer Fig.01. This feature is even more impressive in Fig.09, where the quantities of Fig.08 are also to be seen, however, transformed to the *wave lengths* axis, - in order to link dispersion characteristics additionally to the energy content of the partial waves. (Note that the horizontal axis is shown side-inverted in order to ease comparison with

Fig.08.) Referring to c(AD)(L), the respective deviation is documented by *jumps*. Here there is dc/dL<< 0 tending to the limiting value dc/dL → -∞, while in the wave lengths ranges between the discrete spots of resonance there are *stronger* gradients dc/dL > 0.

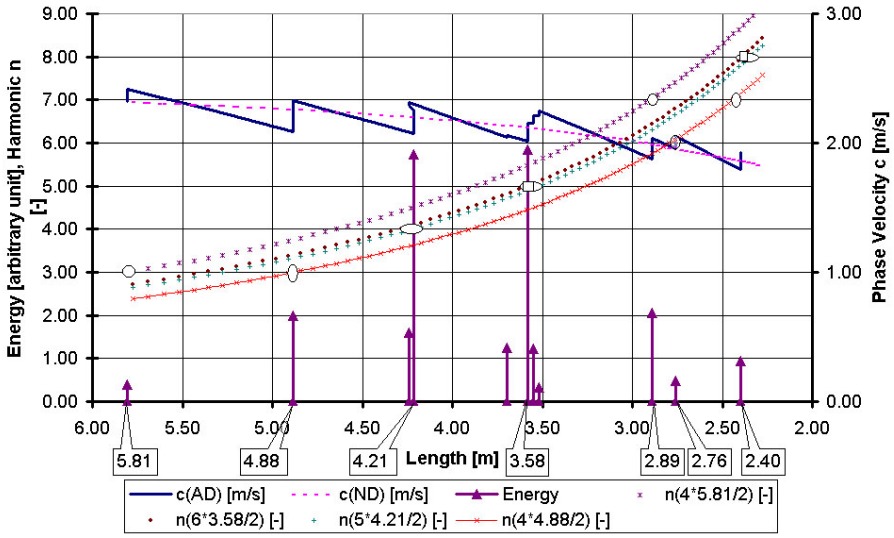

Fig. 09: Phase Velocities c, Harmonic Numbers n_i and Energy Plotted with Lengths of Partial Waves

Additionally the *values of energy* are allotted to the respective lengths of partial waves. It can be seen that maximum energies of nearly equal amount belong to partial wave lengths 4.21m and 3.58m. Calculating the arithmetic mean wave length from *all* partial waves (weighted with the energy) obviously such a wave length corresponds to the resultant partial clapotis length $L_C = 3.65$m found from Fig.04. Finally the 4 functions of oscillatory mode numbers also are plotted as $n_i(L)$ within Fig.09.

STORM WAVE RESONANCES AT A RIDGE COAST

Water level deflections $\eta_{100}(t)$ and $\eta_{85}(t)$ synchronously measured at two locations, 15m distant, on the beach (to be seen from Fig.10) had repeatedly been the matter of analyses carried out by the author previously. (Büsching, 1975, 1976)

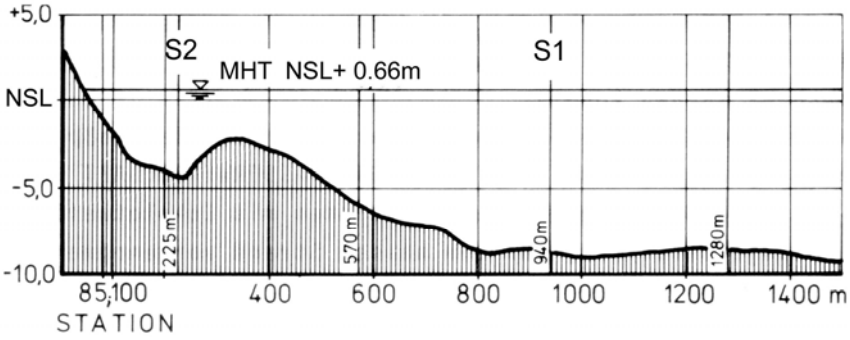

Fig.10: Gage Location at the Beach of Westerland, Sylt Island, 1973.

With regard to the present topic the *phase velocity spectrum c(f)* and basing thereon the *lengths spectrum L(f)*, are of special interest.

$$c(f) = L \cdot f = \frac{\overline{xy}}{\varphi_{xy}(f)/2 \cdot \pi \cdot f} \qquad (04)$$

$$L(f) = \frac{\overline{xy}}{\varphi_{xy}(f)/2\cdot\pi} \qquad (05)$$

where $\overline{xy}$ = 15m = distance between stations x and y in the coast normal control line and $\varphi_{xy}(f)$ = phase difference between the Fourier components of frequencies f_i related to those stations.

As an example all the spectral functions of measurement number 04 (December 13, 1973, 17.00) are placed one beneath another in Fig.11 through 13.
Because of space limitations, only this one out of five similar measurements at water depths $d \geq 3.6$m can be shown here. The remaining measurements are contained in Büsching (2003, 2004).

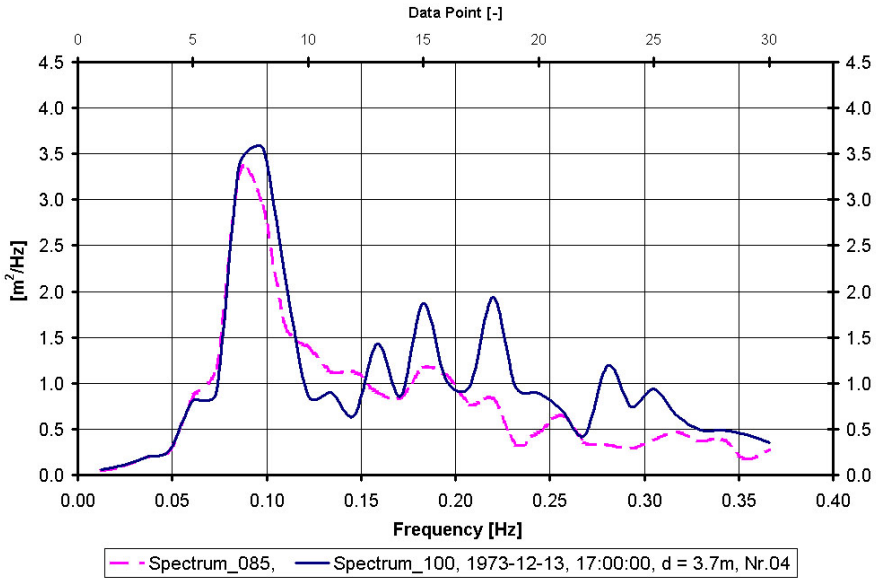

Fig.11. Synchronously Measured Energy Spectra of Storm Waves at Stations 100m and 85m

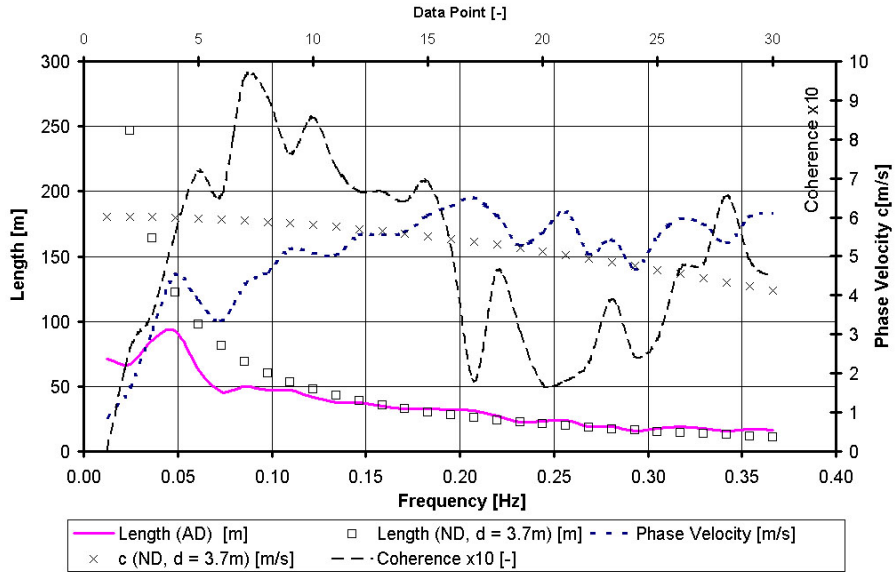

Fig.12. Spectra of Phase Velocities c(f), Lengths L(f) and Coherence

In Fig.11 the considerable peak energy densities suggest that *resonance phenomena* might be effective. Accordingly a *strong anomalous dispersion* is to be seen from the phase velocities at the energy containing frequencies in Fig.12. Moreover the respective

frequency range is *neighbored by portions of stronger normal dispersion*, as it is true to the resonant absorption phenomena of EM-waves and to the wave tank results as well.

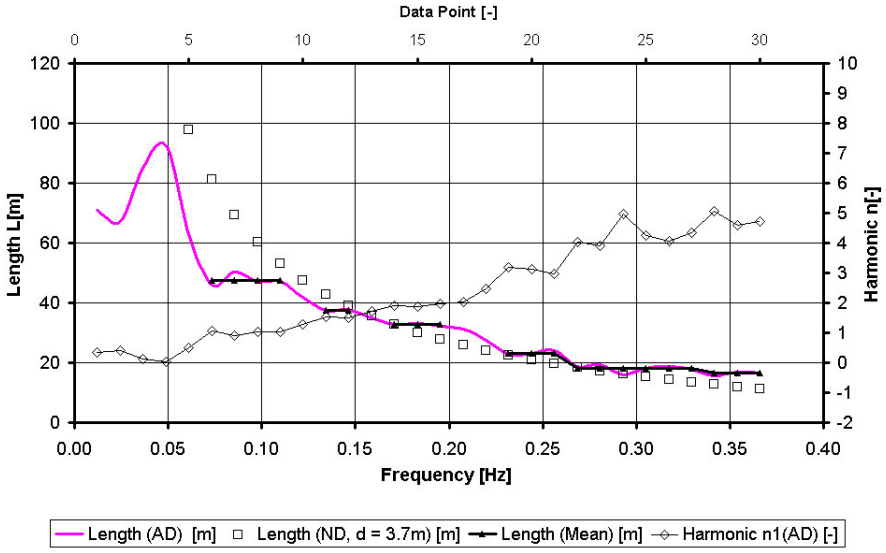

Fig.13. Enlarged Lengths Spectrum L(f) and Harmonic Numbers n_i(f)

Finally also the component wave lengths tend to be *nearly constant* at the respective frequencies, see Fig.12 and Fig.13. Actually the calculated harmonic numbers n[-] in Fig.13 suggest that the peak of the spectrum matches the first harmonic oscillatory mode of the enclosed water body and that higher harmonics (n = 2, 3, 4) as well as the fundamental oscillation (n = 0) might also be present.

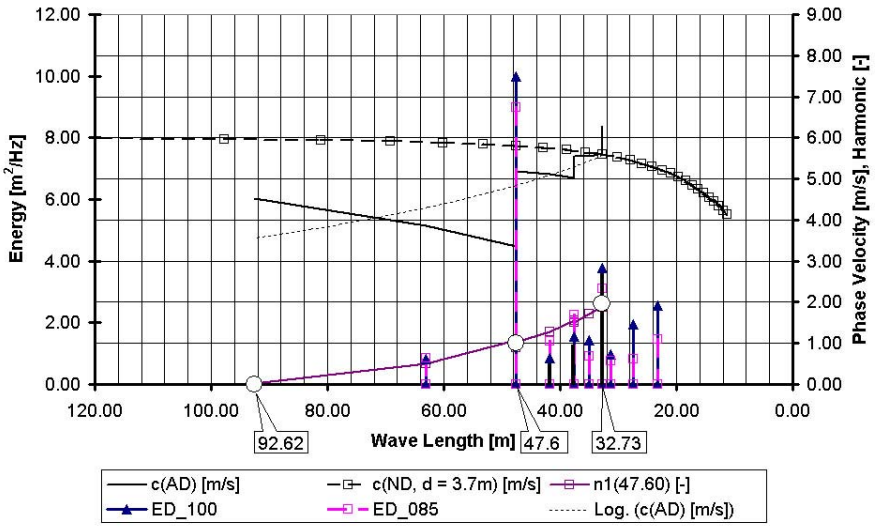

Fig.14. Phase Velocities c(ND)(L) and c(AD)(L), Harmonic Numbers n(L) and Line Spectra of Energy Density ED(L)

Similar to Fig.09 (model investigations) the spectra of phase velocities c(ND)(f) and c(AD)(f) (Fig.12) had been transferred into spectra c(ND)(L) and c(AD)(L) respectively, confer curves in the upper part of Fig.14. c(AD)(L) is shown, however, restricted to the frequency range $0.05Hz \le f \le 0.18Hz$ only, where mean coherence values are big enough (about $\overline{\gamma}^2_{xy} = 0.8$; not shown). As expected in the spectrum c(AD)(L) jumps (dc/dL →- ∞) also appear, by which the higher harmonics can be

identified. The corresponding harmonic numbers n1(L) are shown in the lower part of the figure. Contrary to the model investigations, however, only adjacent to the first harmonic there are stronger gradients dc/dL > 0 compared to that of c(ND, d = 3.7m), while the total trend is dc/dL < 0, representing anomalous dispersion. Finally in Fig.14 and Fig.15 the *line spectra* of energy densities ED(L) are plotted with reference to stations 100m and 85m.

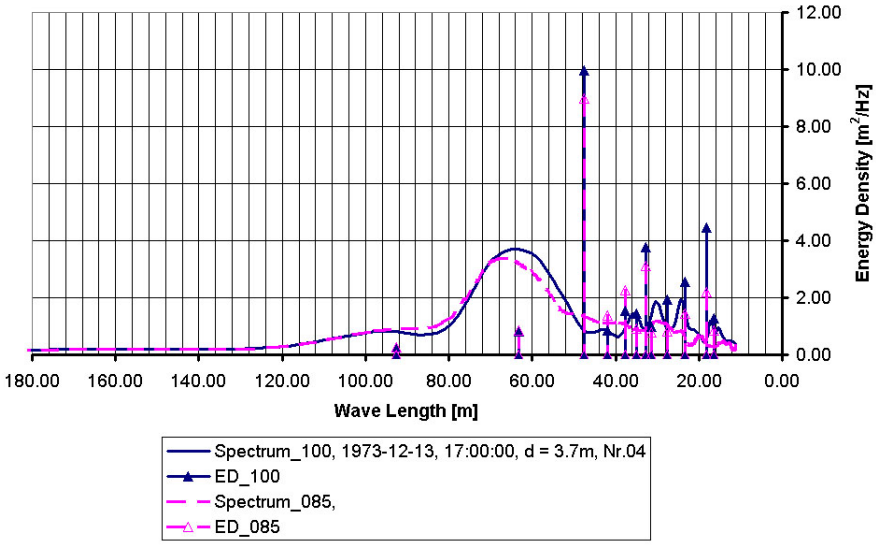

Fig.15. Energy Density Spectra Transferred to the Length Axis and Line Spectra of Energy Density ED(L)

Such spike values of energy density, related to discrete wave lengths, had been calculated by summing up the single amounts of energy densities of frequency components comprising of (nearly) equal wave lengths. With reference to station 100m the maximum energy density maxED(L) ≈ 10m2/Hz belongs to a wave length LP(AD) ≈ 48m. By contrast in the continuous frequency spectrum there is a maximum energy density of about maxEP(f) ≈ 3.6m2/Hz and applying classical normal dispersion the corresponding wave length is LP(ND) ≈ 63m >> LP(AD) ≈ 48m, see Fig.15. Actually such smaller wave lengths had been found applying zero crossing evaluation method on the respective analogue wave data.

SUMMARY OF FINDINGS

Resonance in a Wave Tank due to Re-reflection

- Different resonant seiching modes existing in a wave tank at the same time are characterized by the kinematics of partial standing waves (→ partial waves).
- *Partial waves* are composed of a number of neighbouring frequency components marked by approximately *equal wave lengths* and by this reason comprise of an anomalous dispersion property.
- Different resonant seiching modes can be understood as an ensemble of resonators absorbing energy densities from the input spectrum.

Storm Wave Resonance at a Ridge Coast

- *Wave lengths spectra L(f)*, calculated from measured anomalous phase speed spectra c(f), in general show smaller wave lengths at energy containing frequencies and comprise of a wavy or stepped structure.
- Different resonant seiching modes existing in the trough between sand bar and the beach at the same time correspond to neighbouring frequency components

comprising of nearly equal component lengths. They can be arranged as a kind of *line spectra* ED(L) and be allotted to the geometry of the trough.

- Resonance absorption and anomalous dispersion form a combined phenomenon even with reference to water bodies enclosed *imperfectly*.
- There is an analogy in the general dispersion properties of gravity waves moving in water bodies enclosed imperfectly and of electromagnetic waves passing through dielectrics.

REFERENCES

Heathershaw, A.D. 1982. Seabed-wave resonance and sand bar growth. *Nature Vol. 296,* pp. 343-345.

Mei, C.C. 1989 Applied Dynamics of Ocean Surface Waves, World Scientific, Singapore 700pp

Büsching, F. 1976. On Energy Spectra of irregular Surf Waves, Proceedings, 15th Internat. Conference on Coastal Eng., Honolulu, Hawaii, USA, pp. 539-559

Büsching, F. 1978. Anomalous Dispersion of Surface Gravity Waves in the Near Shore Zone, Proceedings 16th International Conference on Coastal Eng., Hamburg, pp. 21

Büsching, F. 1992. Wave and Downrush Interaction on Sloping Structures, Proc. 10th International Harbour Congress, Antwerpen, pp. 5.17-5.25

Büsching, F. 2001. Combined Dispersion and Reflection Effects at Sloping Structures, Proc. On Port and Maritime R&D and Technology, Vol.I pp. 411-418, Singapore

Büsching, F. 2003. Storm Wave Resonance Controlled by Hollow Block Structures, COPEDEC VI, Colombo, Sri Lanka, CD Proceedings: Paper No.90 p.1-20.

Büsching, F. 2003. Sturmwellen-Resonanz an der Westküste der Insel Sylt, Die Küste, Heft 67, pp. 51-82.

Excerpt of chapter 3 from:

Büsching, F.: PHASE JUMP DUE TO PARTIAL REFLECTION OF IRREGULAR WATER WAVES AT STEEP SLOPES,
Proceedings on the Third International Conference on the Application of Physical Modelling to Port and Coastal Protection, COASTLAB 10, Barcelona, Spain, 28th to 30th September, 1st October 2010, Paper 67, p. 1-9.

3. Resonant basin oscillations

As mentioned above, the described data treatment had originally been applied with respect to the analysis of resonant basin oscillations (Büsching, 2005). This topic is, however, taken up here again, because the *existence of a phase jump* would lead to modified boundary conditions to be considered.

Differing from the author´s previous estimate (Büsching 2005), the natural frequencies of a basin, comprising a steep slope at the one end and a rigid flap type wave generator at the other, can obviously be calculated based on boundary conditions corresponding to an *uneven number of quarter-wave lengths*, see Fig. 9:

$$f[Hz] = (2n+1)\cdot\frac{c}{4\cdot D} \qquad [1]$$

where,
D = horizontal distance between the hinge of the wave paddle and IP at the slope,
c = wave celerity and
n = harmonic number.
n = 0 denotes the fundamental oscillation and n = 1, 2, 3 ... are named first, second, third harmonic etc.

Solving formula [1] with respect to harmonic numbers n[-], yields formula [2]:

$$n(f)[-] = \frac{2\cdot D\cdot f}{c} - 0{,}5 \qquad [2]$$

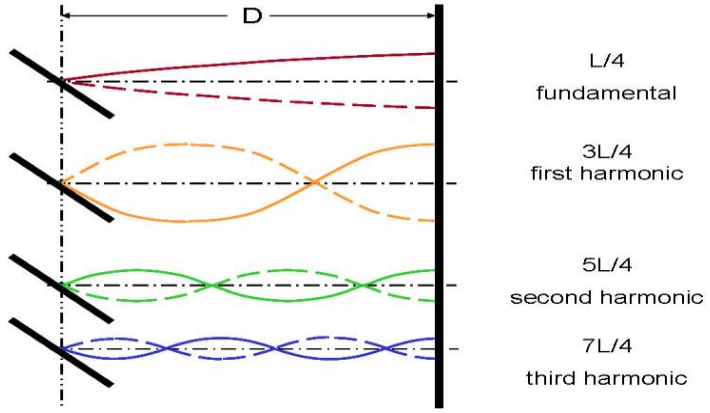

Figure 9. The first 4 theoretical mode shapes of natural oscillations in a basin confined by a vertical wall at the front end and an inclined wall at the rear end.

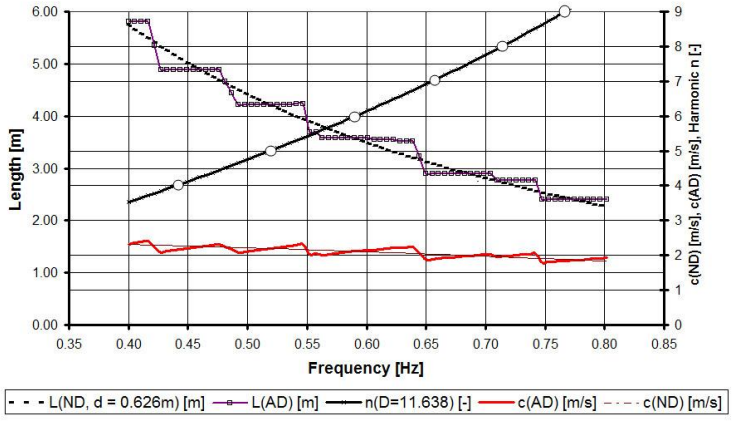

Figure 10. Component length L, phase velocities c and harmonic numbers n plotted with frequency.

Thus the present contribution provides the opportunity to improve some former findings on the harmonics, found in the wave tank.
With the horizontal distance D = 11.638m (between IP and the hinge of the wave maker) in formula [2], it is evident in Fig.10 that partial waves actually occurred as harmonics of ordinal numbers $4 \le n \le 9$. It is to be seen that the integer harmonic numbers correspond rather well to the frequency ranges, in which neighbouring component waves have (almost) equal wave lengths (according to Fig.05). Especially they are centred around the *mean* frequencies of partial waves with wave lengths 3.58m and 4.21m, which both carry maximum energies.

Moreover, the *anomalous dispersion* property of neighbouring frequency components is demonstrated in Fig.10. Due to the fact that the frequency components of the partial waves have nearly equal wave length, follows that there is an *anomalous dispersion* property within such wave packets, because the phase velocity, according to $c = L\cdot f$, increases with frequency. It is $dc/df > 0$.

In the upper part of Fig.10 the lengths associated with the 82 energy lines, mentioned above, are denoted L(AD)(f) (AD = anomalous dispersion), whereas L(ND)(f) (ND = normal dispersion; dashed line) refers to the classical dispersion relation according to water depth d = 0.626 m in the wave tank.

Thus, both curves can be named Length Spectra. Besides the mentioned (red) phase velocity spectrum c(AD)(f) also the theoretical phase velocity spectrum c(ND)(f), derived from

$$\omega^2 = g \cdot k \cdot \tanh(k \cdot d) \qquad [3]$$

is shown in the lower part of the figure.

Hence, the combined appearance of *resonance* and *anomalous dispersion*, known from electromagnetic waves, might also be valid in this context.

Büsching, F. 2010 (a): Phase Jump Due to Partial Reflection of Irregular Water Waves at Steep Slopes, Complete Version, 25pp. Coastlab10, Barcelona, Spain, Paper number 67. urn:nbn:de:0066-201011099 http://hydromech.de/Veroeff/phase_jump_20101109.pdf

Büsching, F. 2010 (b): Phase Jump Due to Partial Reflection of Irregular Water Waves at Steep Slopes, PowerPoint 25 slides. Coastlab10, Barcelona, paper number 67. urn:nbn:de:0066-201011165 http://hydromech.de/Veroeff/phase_jump_20101116.pdf

Büsching, F. 2010: Phasensprung bei der partiellen Reflexion irregulärer Wasserwellen an steilen Uferböschungen, 1. HANSA – International Maritime Journal ISSN 0017-7504, C 3503 E, 147, H. 5 p.87-98, 2010. 2. Binnenschifffahrt ISSN 0939-1916, C 4397 D, 65, H.9 p.73-77 & H.10, p. 64-69.